Journal of University of Science and Technology Beijing
Volume 12, Number 6, December 2005, Page 545

Materials

Corrosion behaviors of zinc and Zn-Ni alloy compositionally modulated multilayer coatings

Jingyin Fei, Guozheng Liang, Wenli Xin, Weikang Wang, and Jianghong Liu

Department of Applied Chemistry, Northwestern Polytechnical University, Xi'an 710072, China
(Received 2004-12-29)

Abstract: Zinc and Zn-Ni alloy compositionally modulated multilayer (CMM) coatings were electrodeposited from dual baths. The coated samples were evaluated in terms of surface appearance, surface and cross-sectional morphologies, as well as corrosion resistance. The results obtained from the salt spray test show that the zinc and Zn-Ni alloy CMM coatings are more corrosion-resistant than the monolithic coatings of zinc or Zn-Ni alloy alone with a similar thickness. The corrosion potential measurement and anodic polarisation tests were undertaken to examine the probable corrosion mechanisms of zinc and Zn-Ni alloy CMM coatings. Analysis on the micrographic features of zinc and Zn-Ni alloy CMM coatings after the corrosion test explains the probable reasons why the Zn-Ni/Zn CMM coatings have a better protective performance. Surface morphologies and compositional analysis of the remaining coating material of Zn-Ni alloy deposit after the corrosion test confirms the dezincification mechanism of the Zn-Ni alloy deposit during the corrosion process.

Key words: electrodeposition; Zn-Ni alloy; compositionally modulated multilayer coatings

1 Introduction

As a sacrificial coating for ferrous substrates under normal atmospheric conditions, zinc provides good protection to steel substrates. Nevertheless, such coatings deteriorate and are consumed quickly in severely corrosive environments. Increasing the thickness of zinc coatings on steel may enhance corrosion resistance, but it can also cause problems during the forming and welding of steel [1]. Consequently, in the past decades several attempts have been made to develop highly corrosion-resistant coatings. The development of zinc-based alloys has been of much interest for the protection of steel substrates. Commonly electrodeposited zinc alloys are usually Zn-Fe, Zn-Ni, Zn-Co, Zn-Mn and Zn-Sn alloys [2-6]. Amongst them, the Zn-Ni alloy has been studied extensively and put into practical use in the mass production of steel sheets for automobile bodies and also small components such as nuts and bolts *etc.* [7-8]. Despite that the development of the Zn-Ni alloy coatings has produced a large improvement over the pure zinc coatings for the protection of steel substrates, further development for getting even better protective properties is of distinct commercial interest. Maybe a relatively new electrodeposited coating class called compositionally modulated multilayer (CMM) coatings was a possible further route to enhance the efficacy of simple monolithic Zn-Ni alloy coatings [9]. CMM coatings consist of a large number of thin alternate metal layers or alloy layers, and each layer has its own distinctive role in achieving preferred performances. The development of zinc-based CMM coatings for the protection of steel substrates has been the keen subject of much research recently [10-14]. Zinc and nickel CMM coatings electrodeposited from dual baths showed enhanced anti-corrosion performance [13-14]. Previous work undertaken by us on layered coatings formed by layering zinc with nickel from revised dual baths also showed the enhanced corrosion protection, assessed mainly by neutral salt spray corrosion test [15-16]. However, little work has been done on the corrosion performance of zinc and Zn-Ni alloy CMM coatings to date, and relatively few papers were reported on the electrodeposition of zinc and Zn-Ni alloy CMM coatings. The aim of the present work is to investigate the probable corrosion mechanism of zinc and Zn-Ni alloy CMM coatings using mainly neutral salt spray testing, corrosion potential measurement, and anodic polarization methods.

2 Experimental

The substrate for electroplating was mild steel panels (with a plated area of 4 cm×4 cm). The pretreatment before plating consisted of an initial soak in an alkaline cleaner (40 $g \cdot L^{-1}$ sodium carbonate +5 $g \cdot L^{-1}$ sodium hydroxide) at 60°C for 5 min, followed by rinsing in tap water, then degreasing by using cathodic cleaning in a solution containing 25 $g \cdot L^{-1}$ sodium car-

Corresponding author: Jingyin Fei, **E-mail:** jyfei@nwpu.edu.cn

creasing the thickness of sublayers). No micro-cracks existed in the Zn-Ni alloy sublayers with an individual layer thickness equal to or less than 2 μm may be one of the reasons why zinc and Zn-Ni alloy CMM coatings with an individual layer thickness of 2 μm exhibits a better protection performance than that of the zinc and Zn-Ni alloy CMM coatings with an individual layer thickness of 3 μm or Zn-Ni alloy monolithic coatings with the same total thickness (12 μm).

Figure 1 Surface morphologies of zinc and Zn-Ni alloy CMM coatings: (a) Zn-Ni3/Zn3 CMM coating; (b) Zn-Ni2/Zn2 CMM coating; (c) Zn3/Zn-Ni3 CMM coating; (d) Zn2/Zn-Ni2 CMM coating (Terminology for CMM coatings: X/Y CMM coatings, commencing with X sublayer, finishing with Y sublayer. Numbers following the metals are the sublayer thicknesses in μm).

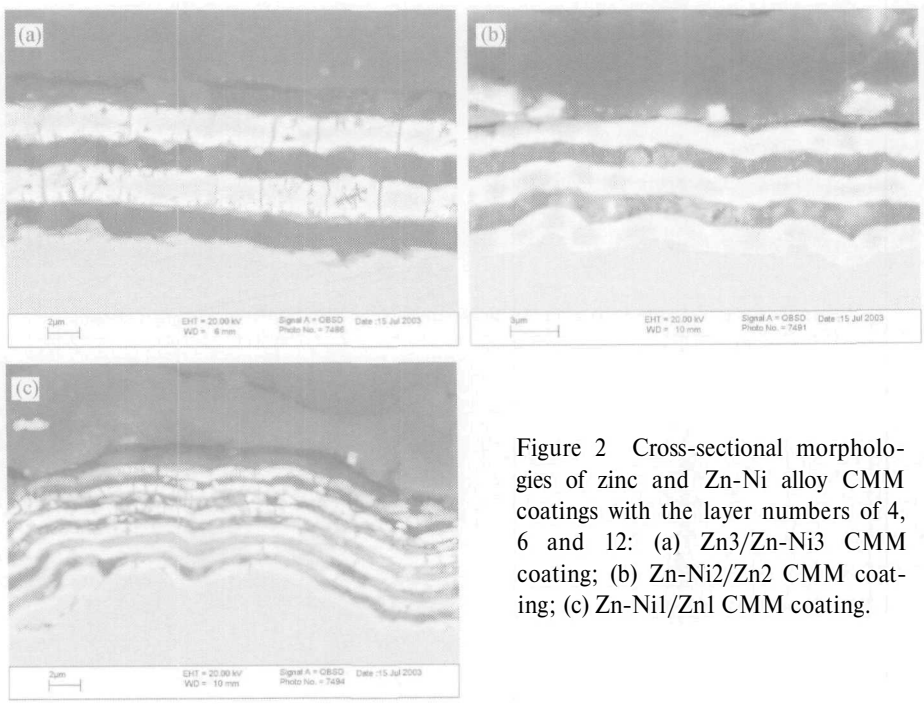

Figure 2 Cross-sectional morphologies of zinc and Zn-Ni alloy CMM coatings with the layer numbers of 4, 6 and 12: (a) Zn3/Zn-Ni3 CMM coating; (b) Zn-Ni2/Zn2 CMM coating; (c) Zn-Ni1/Zn1 CMM coating.

3.2 Neutral salt spray (NSS) test

The coated zinc and Zn-Ni alloy CMM samples were evaluated for their corrosion performance by neutral salt spray test (in accordance with ASTM B117). The results of the salt spray test are shown in **figure 3.** The surface of bare steel plates developed red rust corrosion product over the whole surface after 4 h of test. The time to the first red rust for zinc and

creasing the thickness of sublayers). No micro-cracks existed in the Zn-Ni alloy sublayers with an individual layer thickness equal to or less than 2 urn may be one of the reasons why zinc and Zn-Ni alloy CMM coatings with an individual layer thickness of 2 μm exhibits a better protection performance than that of the zinc and Zn-Ni alloy CMM coatings with an individual layer thickness of 3 μm or Zn-Ni alloy monolithic coatings with the same total thickness (12 μm).

Figure 1 Surface morphologies of zinc and Zn-Ni alloy CMM coatings: (a) Zn-Ni3/Zn3 CMM coating; (b) Zn-Ni2/Zn2 CMM coating; (c) Zn3/Zn-Ni3 CMM coating; (d) Zn2/Zn-Ni2 CMM coating (Terminology for CMM coatings: X/Y CMM coatings, commencing with X sublayer, finishing with Y sublayer. Numbers following the metals are the sublayer thicknesses in μm).

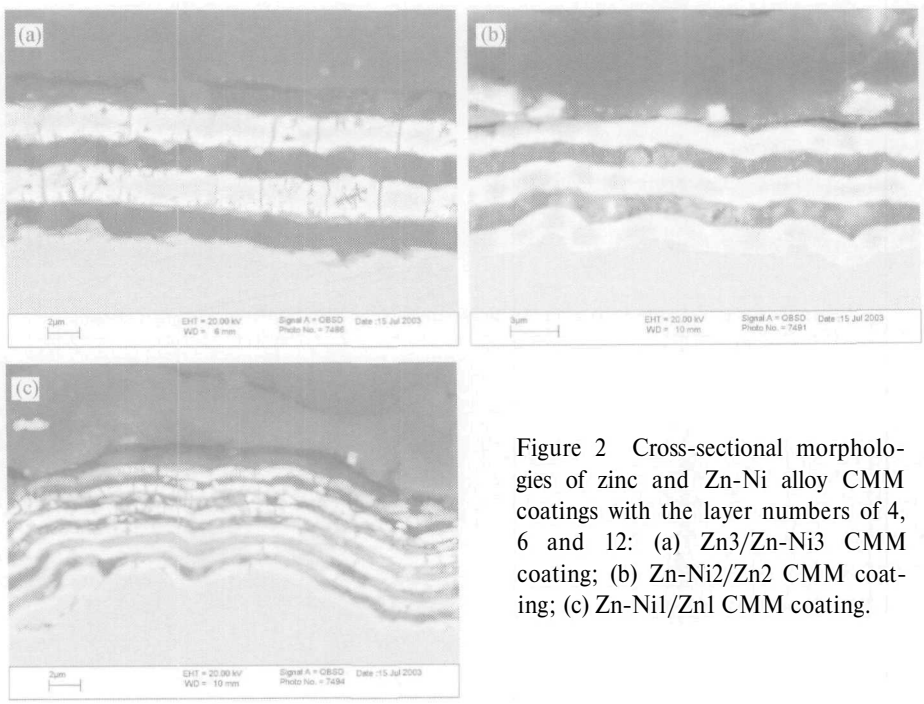

Figure 2 Cross-sectional morphologies of zinc and Zn-Ni alloy CMM coatings with the layer numbers of 4, 6 and 12: (a) Zn3/Zn-Ni3 CMM coating; (b) Zn-Ni2/Zn2 CMM coating; (c) Zn-Nil/Znl CMM coating.

3.2 Neutral salt spray (NSS) test

The coated zinc and Zn-Ni alloy CMM samples were evaluated for their corrosion performance by neutral salt spray test (in accordance with ASTM B117). The results of the salt spray test are shown in **figure 3.** The surface of bare steel plates developed red rust corrosion product over the whole surface after 4 h of test. The time to the first red rust for zinc and

Zn-Ni alloy plated steel panels was 48 and 288 h, respectively. All the zinc and Zn-Ni alloy CMM coatings showed a longer time to red rust than that of zinc or Zn-Ni alloy deposits with a similar overall thickness (12 μm). Moreover, the steel substrates coated with a Zn-Ni/Zn CMM coating system usually had a much longer time to red rust than those coated with a Zn/Zn-Ni alloy CMM coating system. These results illustrate a similar pattern to that of zinc and nickel alternate multilayers reported elsewhere [14]. The results also showed that, for either Zn-Ni/Zn or Zn/Zn-Ni CMM coating system, the zinc and Zn-Ni alloy CMM coatings with an individual sublayer thickness of 2 μm had the longest time to red rust amongst all the samples tested. This may be attributed to the less defects in the 2 μm sublayers, because more microcracks existed in the Zn-Ni alloy sublayers with an individual thickness lager than 3 μm, and the higher porosity in the Zn-Ni alloy sublayers with an individual thickness less than 2 μm.

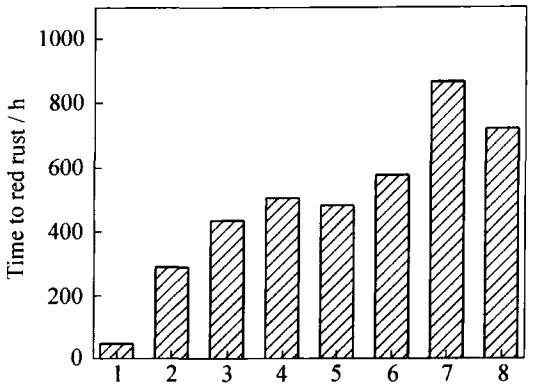

Figure 3 Dependence of corrosion resistance on the zinc and Zn-Ni alloy CMM coating configurations. 1: Znl2; 2: Zn-Nil2; 3: Zn3/Zn-Ni3; 4: Zn2/Zn-Ni2; 5: Znl/Zn-Nil; 6: Zn-Ni3/Zn3; 7: Zn-Ni2/Zn2; 8: Zn-Nil/Znl.

3.3 Corrosion **potential measurement**

The relationship between the corrosion potential and coating configuration is illustrated in **table 1.** The corrosion potentials for zinc, Zn-Ni alloy deposits (12 μm) and steel substrate are also presented here for comparison. The Zn-Ni/Zn CMM coating system (No. 4, 5 and 6) shows more consistently low corrosion potentials which is very close to that of the electrodeposited zinc coating (No.2) because of the zinc top layers. Nevertheless, the Zn/Zn-Ni alloy CMM coating system (No.7, 8 and 9) illustrates relatively low (negative) potentials with respect to the single layer Zn-Ni alloy deposit (No.3), suggesting that the Zn-Ni alloy top layer is a little porous, therefore, the mixed potentials of the Zn/Zn-Ni alloy CMM coating system are very close to that of the zinc electrodeposited sample (No.2).

3.4 **Anodic polarization** studies

Anodic polarisation tests were undertaken on zinc and Zn-Ni alloy CMM coatings with different coating configurations and other monolithic coatings and metals at a sweep rate of 2 mV/s from the free corrosion potential. Figure 4 illustrates the anodic polarisation curves for steel substrate, Zn-Ni alloy deposit, zinc coating, and pure zinc foil as well. It is evident that the Zn-Ni alloy shows the smallest initial anodic current amongst the four samples tested, implying that the Zn-Ni alloy is the least active. Curves 1, 3 and 4 are presented here for reference. The corrosion potential (E_{corr}=-843 mV *vs.* SCE) of the Zn-Ni alloy electrodeposited sample is more negative than that of the steel substrate, suggesting that, under the same conditions, Zn-Ni alloy coatings offer sacrificial protection for ferrous substrates, which is in good agreement with that reported by Gavrila *et al.* [18].

Table 1 Dependence of corrosion potentials (E_{corr}) on coating configurations

No.	Coating system	Number of layers	Layer adjacent to the steel substrate	Top layer	E_{corr} /mV *vs.* SCE
1	Fe		Bared Fe	Bared Fe	−566
2	Zn12	1	Zn	Zn	−1045
3	Zn-Ni12	1	Zn-Ni	Zn-Ni	−843
4	Zn-Ni3/Zn3	4	Zn-Ni	Zn	−1025
5	Zn-Ni2/Zn2	6	Zn-Ni	Zn	−1032
6	Zn-Nil/Znl	12	Zn-Ni	Zn	−1035
7	Zn3/Zn-Ni3	4	Zn	Zn-Ni	−1002
8	Zn2/Zn-Ni2	6	Zn	Zn-Ni	−1005
9	Znl/Zn-Nil	12	Zn	Zn-Ni	−1009

Figures 5-7 show the anodic polarisation curves of Zn-Ni/Zn CMM coatings with zinc as the top layer and containing 4, 6 and 12 individual layers, respectively. All of them show a similar profile. A rapidly increasing current at the initial stage corresponds to the dissolution of the zinc top layer. The first current peak is attributed to the combination of dissolution of the zinc top layer and zinc phase or zinc-rich phase

(η-phase) in the Zn-Ni alloy sublayer. Fratesi *et al.* [19] confirmed the existence of a zinc phase in the Zn-Ni alloy deposits in addition to η-, γ-, and a-phases as normally accepted. A small decrease in current after the first peak is due to the removal of zinc top layer and the remaining phase (γ-phase) which exhibits a higher corrosion resistance. Another increase in current at a slightly higher potential is due to the dissolution of zinc sublayer beneath the Zn-Ni alloy. Such a process is repeated once more for the coatings with a greater number of sublayers. For example, curve 3 in figure 5 has two distinct peaks and curve 3 in figure 6 has three distinct peaks. The number of peaks is equal to the number of zinc sublayers in these coatings, suggesting that the peaks result mainly from the dissolution of the zinc top layers and sublayers when they are exposed to the sodium chloride solution because of the dissolution of Zn-Ni alloy layers covering them. However, these features are not always clear if the individual layer thickness is less than 2 μm *(e.g.* curve 3 in figure 7), the peaks become smaller and the number of the peaks is no longer the same as that of zinc sublayers in this multilayer coating. **Figure 8** illustrates the anodic curves of all the Zn-Ni/Zn CMM coatings with zinc as the top layer. It is evident that the corrosion potentials of the Zn-Ni/Zn CMM coatings are almost the same and very close to that of pure zinc foil possibly due to the zinc top layer in spite of the different coating configurations.

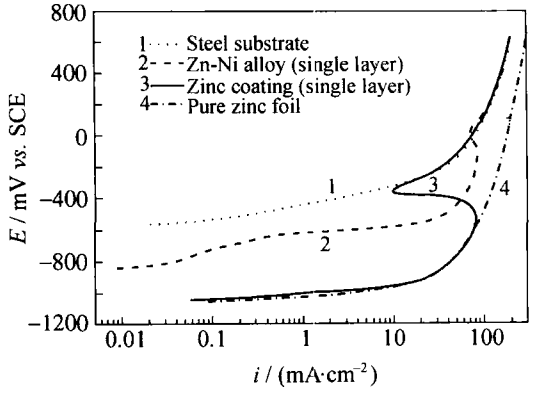

Figure 4 Anodic polarisation curves of tested samples.

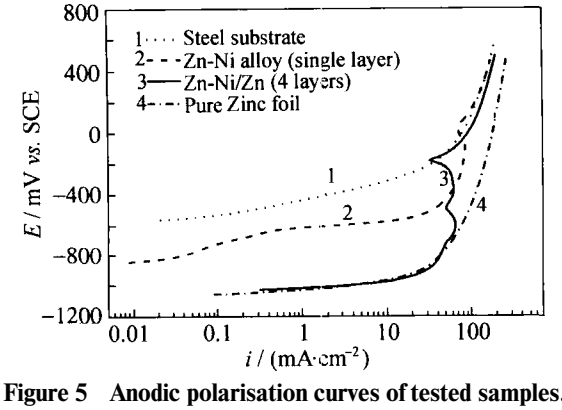

Figure 5 Anodic polarisation curves of tested samples.

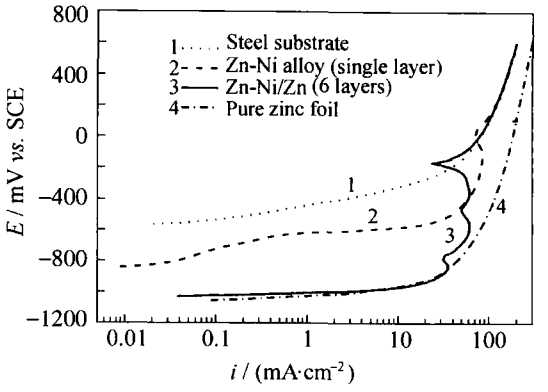

Figure 6 Anodic polarisation curves of tested samples.

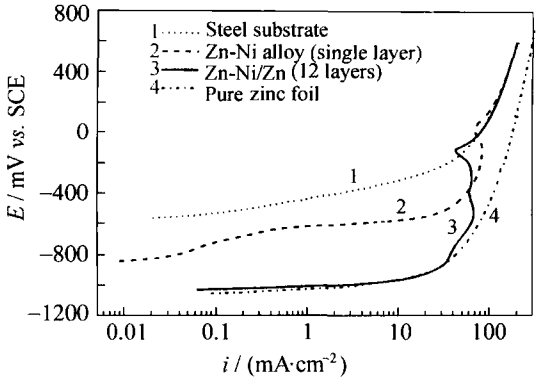

Figure 7 Anodic polarisation curves of tested samples.

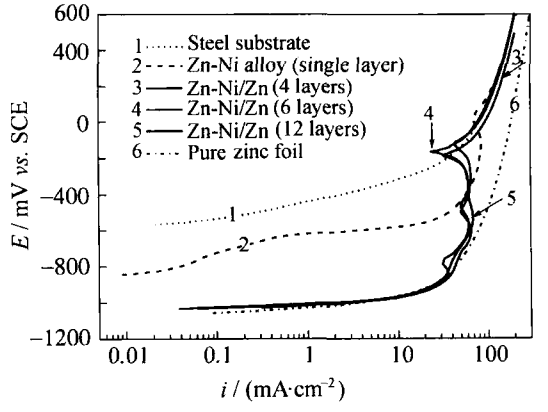

Figure 8 Anodic polarisation curves of tested samples.

Figures 9-11 show the anodic polarisation curves of Zn/Zn-Ni CMM coatings with the Zn-Ni alloy as the top layer and containing 4, 6 and 12 individual layers, respectively, All of them also show a similar profile. A rapid increase in current in curve 3 in figures 9-11 at the initial stage results from the selective dissolution of zinc phase, zinc-rich phase (η-phase) in the Zn-Ni alloy deposits and zinc sublayers through the pores as well. The small peaks at a little more positive potential are associated with the mixed dissolution of the Zn-Ni alloy and zinc sublayer beneath. The increasing current at more positive potential is due to the dissolution of steel substrates. **Figure 12** illustrates the anodic curves of all Zn/Zn-Ni alloy CMM coatings with the Zn-Ni alloy as the top layer. It

is evident that the corrosion potentials of the samples tested are almost the same and very close to that of the pure zinc foil, probably due to the presence of pores in the Zn-Ni alloy top layer in spite of the different coating configurations.

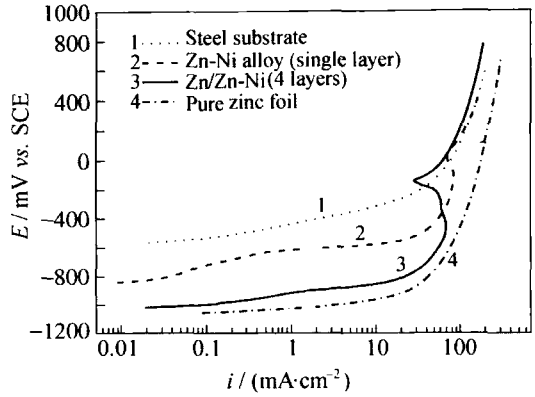

Figure 9 Anodic polarisation curves of tested samples.

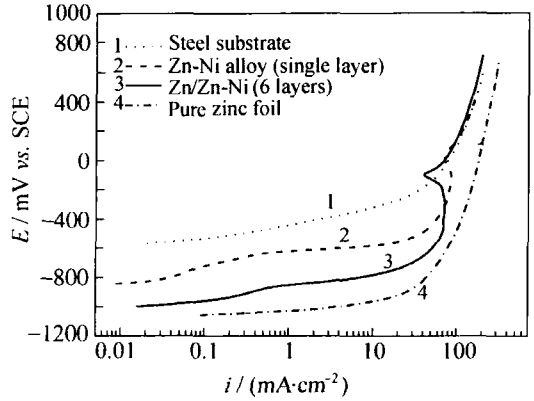

Figure 10 Anodic polarisation curves of tested samples.

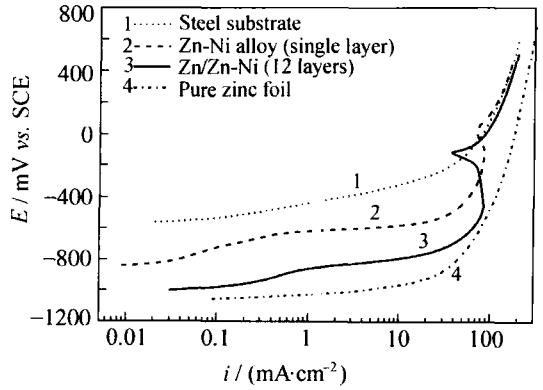

Figure 11 Anodic polarisation curves of tested samples.

3.5 Corrosion mechanism

The corrosion process for Zn-Ni alloy deposits, reported by Short *et al.* [20], was under the anodic control and dezincification led to the forming of an improved barrier layer reducing the rate of anodic dissolution. **Figure 13** shows some surface morphologies of the zinc and Zn-Ni alloy CMM coatings after corrosion test. Sample A commences with the Zn-Ni alloy sublayer adjacent to the steel substrate and finishes with zinc as the top layer (Zn-Ni/Zn CMM coating system), and sample B commences with the zinc layer, and finishes with the Zn-Ni alloy (Zn/Zn-Ni CMM coating system). As shown in these two micrographs, only the individual Zn-Ni alloy sublayers could be found after the corrosion test, which means the zinc sublayers dissolves far more quickly as soon as they are exposed to the corrosion environment when the Zn-Ni alloy sublayers covering them are breached. The marked difference between this two samples lies in that no deposits, neither zinc nor Zn-Ni alloy, remains on the steel surface if the Zn/Zn-Ni CMM coatings is corroded (figure 13 B), while for the Zn-Ni/Zn CMM coating system, there still are some Zn-Ni alloy deposits scattered on the steel substrate, which would provide, to some extent, protection for steel substrates. This accounts for the better corrosion resistance provided by the Zn-Ni/Zn CMM coating system presented above.

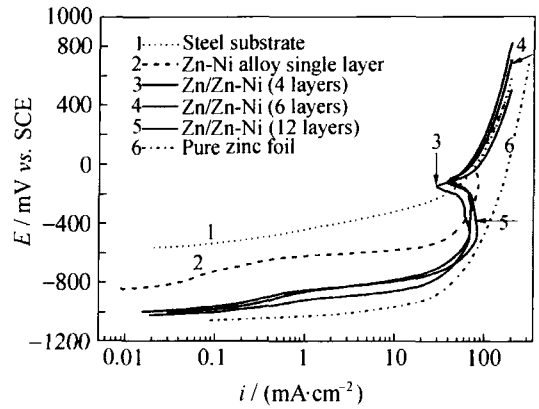

Figure 12 Anodic polarisation curves of tested samples.

Figure 14 shows the surface morphologies of the Zn-Ni alloy coating electrodeposited on to the steel substrate after corrosion test. The surface of the Zn-Ni alloy deposit without corrosion, marked as a, displays a smooth, uniform and crack-free morphology, whereas the corroded area, marked as b, shows the morphology of a 'dried riverbed' cracked structure. The emergence of micro-cracks during the corrosion process reveals that stress exists in the Zn-Ni alloy deposits. Compositional analysis using EDA in areas a and b confirms that the zinc or zinc-rich phase (η-phase) dissolves preferentially since the nickel content is 14wt% in area a and 39wt% in area b. The surface morphology of the corroded area (area b) with a higher magnification is shown in figure 14 B for understanding the selective dissolution of the zinc or zinc-rich phase in the Zn-Ni alloy deposit.

4 Conclusions

(1) The surface appearance, surface and cross-

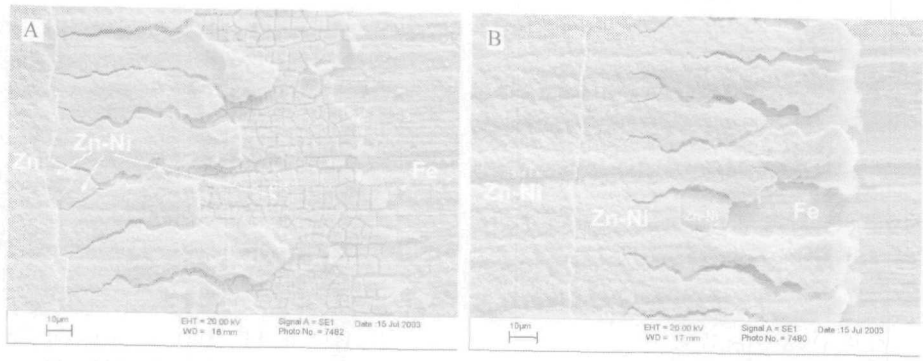

Figure 13 Surface morphologies of zinc and Zn-Ni alloy CMM coatings. A: Zn-Ni2/Zn2 CMM coating; B: Zn2/Zn-Ni2 CMM coating.

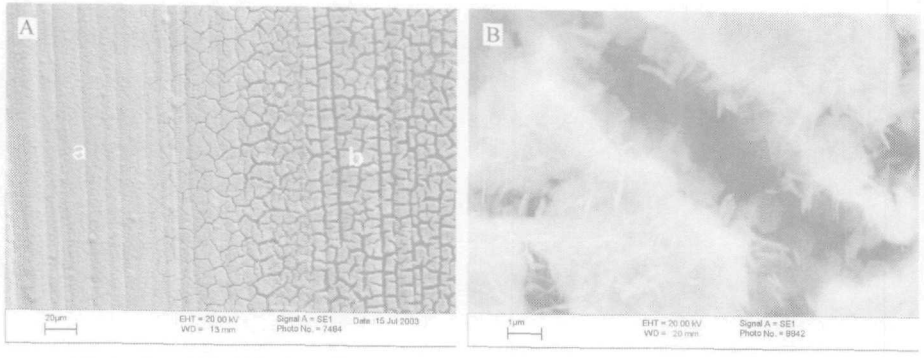

Figure 14 Surface morphologies of Zn-Ni alloy after corrosion test. A: tested sample (with low magnification); B: corroded area (with high magnification).

sectional morphologies of zinc and Zn-Ni alloy CMM coatings examined using FEGSEM show that the zinc and Zn-Ni alloy CMM coatings with fine-grained and more compact crystal structures can be electrodeposited from dual baths.

(2) The corrosion resistance of zinc and Zn-Ni alloy CMM coatings evaluated using neutral salt spray test is much better than that of single-layer zinc or Zn-Ni alloy deposit of a similar thickness, and the Zn-Ni/Zn CMM coatings are more corrosion resistant than that of the Zn/Zn-Ni alloy CMM coatings with a similar structure.

(3) The results obtained from cross-sectional morphologies, corrosion potential measurement, and anodic polarisation tests suggest that internal stress exists in the Zn-Ni alloy and it can be reduced by laying the Zn-Ni alloy with zinc deposit.

(4) Morphological characteristics examined using FEGSEM after the corrosion test show more information on the corrosion mechanism which can be used to explain, to some extent, the reasons why Zn-Ni/Zn CMM coatings have a better corrosion resistance.

Acknowledgements

The author, Jingyin Fei, would like to thank the Chinese Scholarship Council and the Northwestern Polytechnical University for their financial support during his sabbatical visit to Loughborough University.

References

[1] S.A. Watson, Zinc-nickel Alloy electrodeposited steel coil and other pre-coated coil for the use by the automotive industry, [in] *Nickel Development Institute Review,* Series No.13001, Nickel Development Institute, European Technical Information Centre, Birmingham, 1988.

12] Y. Liao, D.R. Gabe, and G.D. Wilcox, A study of zinc-iron alloy electrodeposition using a rotating cylinder hull cell, *Plat. Surf. Finish.*, 85(1998). No.3, p.60.

[3] A. Abibsi, J.K. Dennis, and N.R. Short. The effect of plating variables on zinc-nickel alloy electrodeposition, ***Trans.*** *Inst. Met. Finish.*, 69(1991), No.4, p.145.

[4] J.B. Bajat, V.B. Miskovic-Stankovic, and M.V. Maksimovic. Electrochemical deposition and characterization of Zn-Co alloys and corrosion protection by electrodeposited epoxy coating on Zn-Co alloy, ***Electrochim.*** *Acta.* 47 (2002),p.4101.

[5] C. Muller, M. Sarret, and T. Andreu, Zn-Mn alloys obtained using pulse, reverse and superimposed current modulations, *Electrochim.* ***Acta,*** 48(2003), p.2397.

[6] G.D. Wilcox and D.R. Gabe, Electrodeposited zinc alloy coatings, *Corros. Sci.*, 35(1993), **p.1251.**

[7] M. Gavrila, J.P. Millet, H. Mazille, D. Marchandise, and J.M. Cuntz, Corrosion behavior of zinc-nickel coatings, electrodeposited on steel, *Surf. Coat.* ***Technol.,*** 123(2000), p. 164.

[8] N.R. Short, A. Abibsi, and J.K. Nennis, Corrosion resis-

tance of electroplated zinc alloy coatings, *Trans. Inst. Met. Finish.*, 67(1984), No.l, p.73.

[9] D.R. Gabe, Protective layered electrodeposits, *Electrochim. Acta*, 39(1994), p. 1115.

[10] M.R. Kalantary, GD. Wikox, and D.R. Gabe, The production of compositionally modulated alloys by simulated high speed electrodeposition from a single solution, *Electrochim. Acta*, 40(1995), No.11, p. 1609.

[11] M.R. Kalantary, GD. Wilcox, and D.R. Gabe, Alternate layers of zinc and nickel electrodeposited to protect steel, *Br. Corros. J.*, 33(1998), No.3, p.197.

[12] D.R. Gabe and W.A. Green, The mathematical modeling of CMA multilayered coatings, *Surf. Coat. TechnoL*, 105(1998), p. 195.

[13] G Chawa, GD. Wilcox, and D.R. Gabe, Compositional modulated zinc alloy coatings for corrosion protection, *Trans. Inst. Met. Finish.*, 76(1998), No.3, p.117.

[14] J.Y. Fei and GD. Wilcox, Electrodeposition of zinc-nickel compositionally modulated multilayer coatings and their corrosion behaviors, *Surf. Coat. Technol.* (in press).

[15] W.L. Xin, J.Y. Fei, and GZ. Liang, Dual bath electrodeposition of alternate multilayer coatings of zinc and nickel deposits, *Trans. Mater. Heat Treat.*, 25(2005), No.5, p. 1154.

[16] J.Y. Fei, GZ. Liang, and W.L. Xin, The structure and protective properties of zinc and nickel alternate electrodeposits, *Trans. Mater. Heat Treat.*, 25(2005), No.5, p. 1142.

[17] G Roventi, R. Fratesi, R.A. Della, and G Barucca, Normal and anomalous codeposition of Zn-Ni alloys from chloride bath, *J. Appl. Electrochem.*, 30(2000), p.173.

[18] M. Gavrila, J.P. Millet, and H. Mazille, Corrosion behavior of zinc-nickel coatings, electrodeposited on steel, *Surf. Coat. TechnoL*, 123(2000), p. 164.

[19] R. Fratesi and G Roventi, Corrosion resistance of Zn-Ni alloy coatings in industrial production, *Surf. Coat. Technol.*, 82(1996), p.158.

[20] N.R. Short, S. Zhou, and J.K. Dennis, Electrochemical studies on the corrosion of a range of zinc alloy coated steel in alkaline solutions, *Surf. Coat. TechnoL*, 79(1996), p.218.